PNAS
www.pnas.org

Supplementary Information for

TIC236 gain-of-function mutations unveil the link between plastid division and plastid protein import

Jun Fang[a,b,e,1], Bingqi Li[a,b,f,1], Lih-Jen Chen[c], Vivek Dogra[a,g], Shengji Luo[a,b], Wangpin Wu[a,b], Pengcheng Wang[a], Inhwan Hwang[d], Hsou-min Li[c,2], and Chanhong Kim[a,2]

[a] Shanghai Center for Plant Stress Biology and CAS Center for Excellence in Molecular Plant Sciences, Chinese Academy of Sciences, Shanghai 200032, China

[b] University of the Chinese Academy of Sciences, Beijing 100049, China

[c] Institute of Molecular Biology, Academia Sinica, Taipei 11529, Taiwan

[d] Department of Life Sciences, Pohang University of Science and Technology, Pohang, Korea

[e] Present address: Department of Plant Sciences, University of Oxford, Oxford OX1 3RB, United Kingdom

[f] Present address: Max Planck Institute for Molecular Plant Physiology, 14476 Potsdam-Golm, Germany

[g] Present address: Biotechnology Division, CSIR-Institute of Himalayan Bioresource Technology, Palampur 176061, India

[1]J.F. and B.L. contributed equally to this work

[2]To whom correspondence may be addressed. Email: chanhongkim@cemps.ac.cn and mbhmli@gate.sinica.edu.tw

This PDF file includes:

Figures S1 to S7
Table S1
Legends for Datasets S1 to S5

Other supplementary materials for this manuscript include the following:

Datasets S1 to S5

Figure S1. Alignment of protein sequences of Arabidopsis TIC236 and *E. coli* TAMB. The amino acid sequences of TIC236 (protein accession number: NP_180137) and TAMB (protein accession number: NP_418642) were obtained from NCBI (https://www.ncbi.nlm.nih.gov/protein/) and used for alignment using the Basic Local Alignment Search Tool (BLAST, https://blast.ncbi.nlm.nih.gov). Asterisks refer to conserved amino acid residues between proteins, and the mutated residues are highlighted in red. The identity of the two sequences is ~29%.

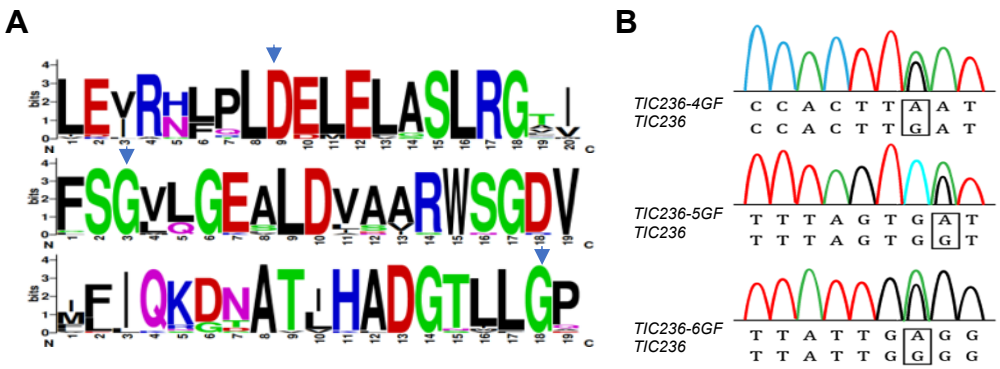

Figure S2. TIC236-GF residues in different plant species and genotyping of *tic236-gf* mutants. A, The TIC236-like protein sequences from 27 plant species reported in Phytozome v12.1 were aligned using ClustalW. The three mutated residues in *spcrl* mutants are indicated with blue arrowheads. Aligned regions were visualized using WEBLOGO. **B,** Sanger DNA sequencing result of *TIC236* mutations in the plants shown in Fig. 1*D*.

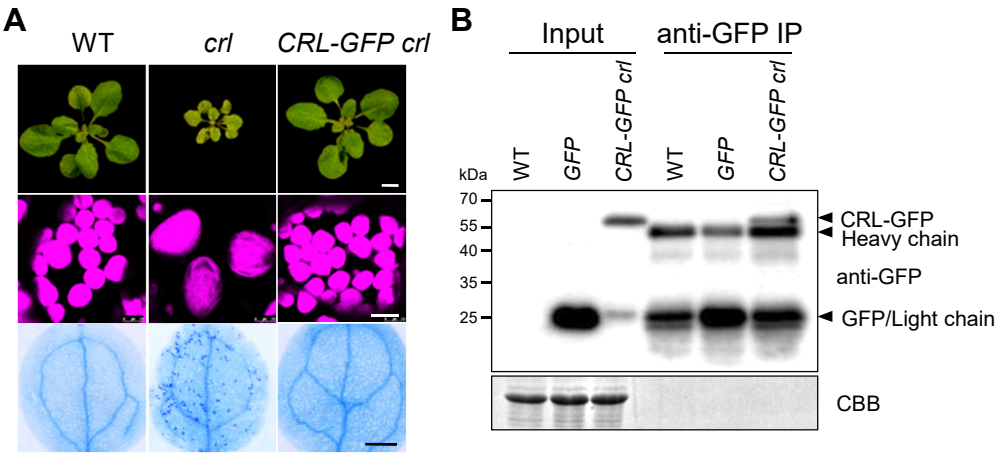

C

Identified Proteins	MW (kDa)	Exclusive unique peptide count					
		GFP			CRL-GFP		
		rep1	rep2	rep3	rep1	rep2	rep3
CRL	30 kDa	0	0	0	13	27	11
TOC75	89 kDa	0	0	4	3	19	18
TOC34	35 kDa	0	0	0	3	3	2
TOC132	132 kDa	0	0	0	0	3	3
TIC110	112 kDa	5	0	0	23	17	8

Figure S3. The biologically active CRL-GFP fusion protein unveils CRL-associated proteins. A, Top: images represent 21-day-old WT, *crl*, and *35S::CRL-GFP crl* (*CRL-GFP crl*) plants. Scale bar, 5 mm. Middle: confocal images of chlorophyll autofluorescence of 5-day-old cotyledons (scale bar, 10 μm). Bottom: localized cell death in 10-day-old cotyledons, as visualized by TB staining (scale bar, 0.5 mm). **B**, Western blot of Co-IP using 14-day-old WT, *35S::GFP* (*GFP*), and *CRL-GFP crl* plants. GFP-conjugated Dynabeads were used to pull down CRL-GFP and its associated proteins. The proteins were subjected to MS analysis after digestion. In parallel, equal amounts of proteins were used for Western blot analysis. Heavy and light chains of the GFP antibody are indicated. Equal protein loading is shown by CBB staining. **C**, List of proteins showing TOC and TIC components, together with CRL, which were detected at least twice in the eluates from *CRL-GFP crl* but not in *GFP* samples.

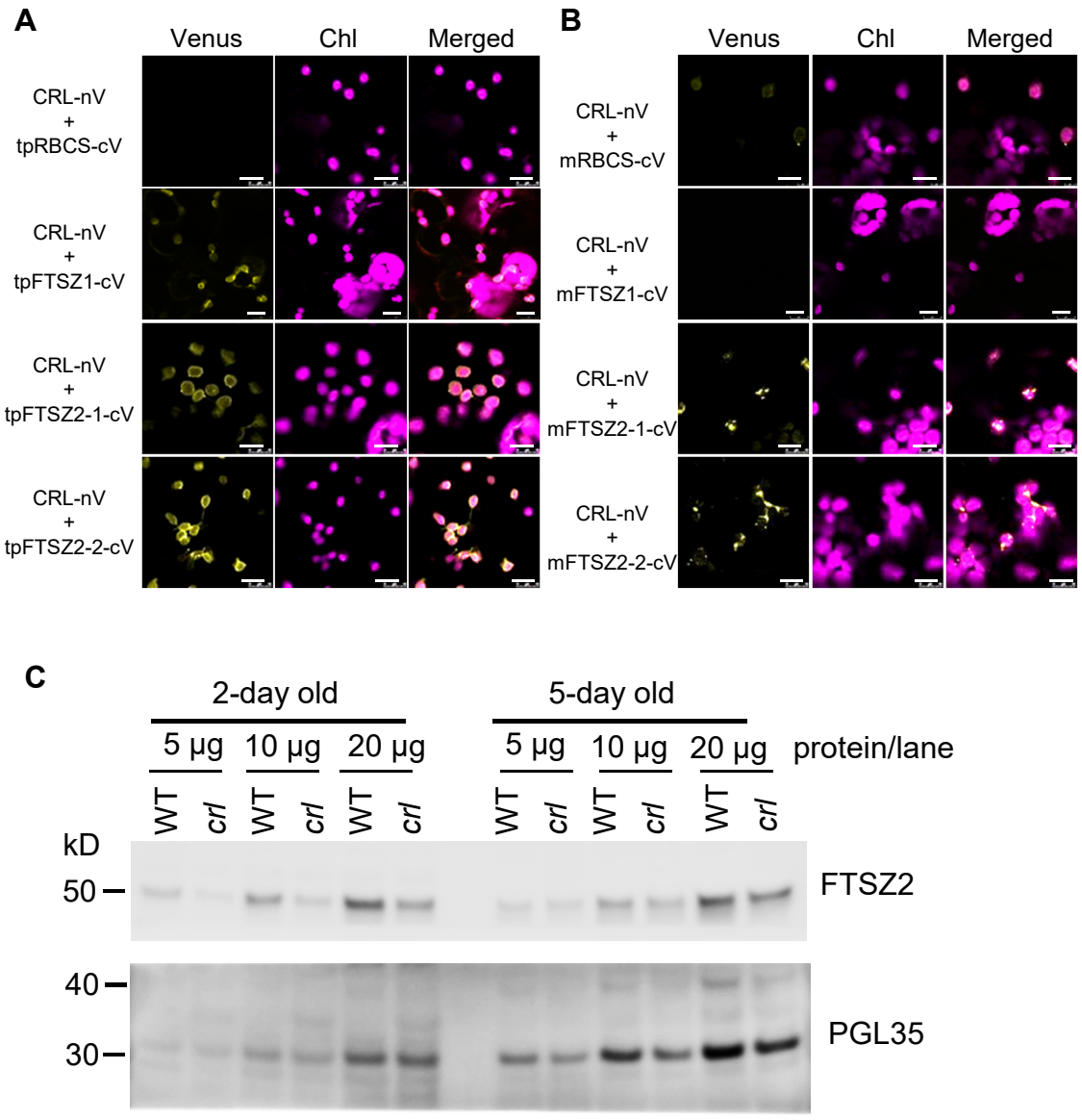

Figure S4. CRL interacts with transit peptides of FTSZ proteins and the amounts of FTSZ2 family proteins were reduced in *crl* in 2-day-old seedlings. A and **B**, Split-Venus constructs of CRL and the transit peptide (tp) lacking mature protein region (**A**) or tp-deleted mature protein (m) (**B**) of either RBCS, FTSZ1, FTSZ1, FTSZ2-1, or FTSZ2-2 were transiently coexpressed in *N. benthamiana* leaves. Fluorescence signal of the integrated Venus protein was monitored by confocal microscopy. Scale bar, 10 μm. (**C**) Steady-state levels of FTSZ2 family proteins. Total proteins were extracted from wild-type (WT) and *crl* mutant seedlings grown on medium (1x MS and 2% sucrose and 16 h light/8 h dark) for 2 days or 5 days and were used for immunoblotting. Plastid PGL35 (PLASTOGLOBULIN 35, also called Fibrillin, At4g04020) was detected as a control.

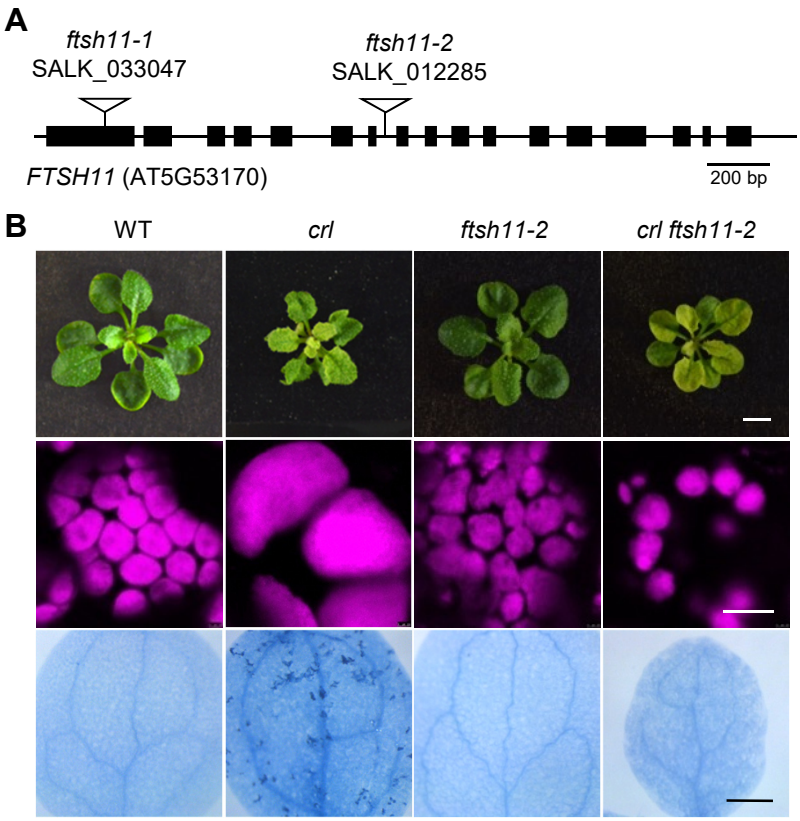

Figure S5. The *ftsh11-2* allele *of ftsh11* mutants also significantly suppresses *crl* phenotypes. A, Schematic representation of the FTSH11 gene (accession number: AT5G53170). Exons and introns are shown as black boxes and black lines between exons, respectively. The inverted triangles indicate the T-DNA insertion sites of the *ftsh11-1* (SALK_033047) and *ftsh11-2* (SALK_012285) mutants. **B**, Top: representative plant images of 21-day-old WT, *crl*, *ftsh11-2*, and *crl ftsh11-2* are shown (top panel). Middle: confocal images of chlorophyll signals from mesophyll cells (scale bar, 10 μm). Bottom: cell death in cotyledons, as visualized via TB staining (Scale bar, 0.5 mm).

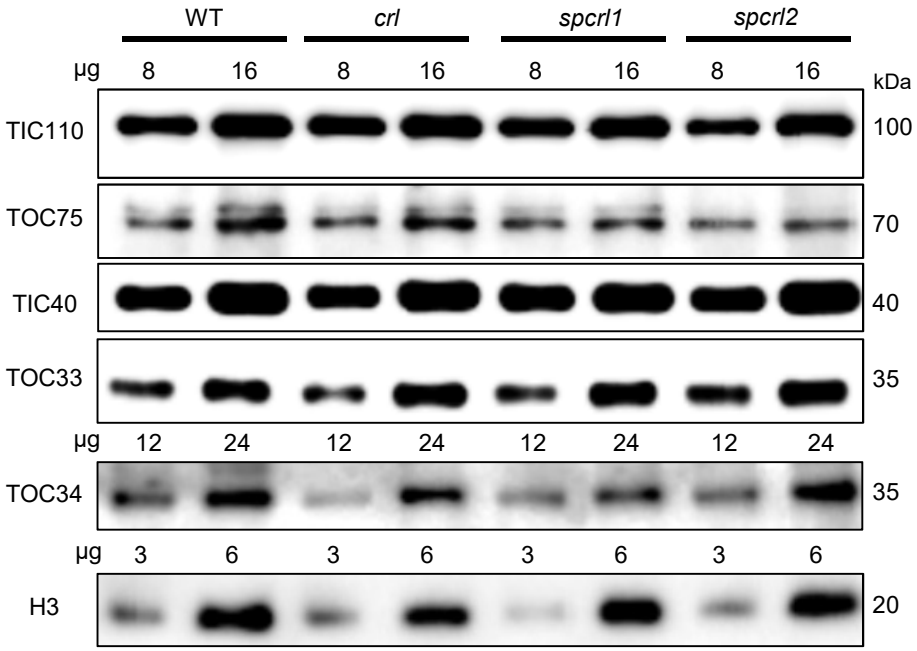

Figure S6. The *crl* mutant phenotypes were not caused by reduced translocon protein levels. Immunoblot analyses of total proteins extracted from 5-day-old seedlings. The amount of proteins loaded is indicated above the lane. The same amounts of proteins were loaded to examine the relative abundance of TIC110, TOC75, TIC40, and TOC33 proteins. H3 protein was used as a loading control.

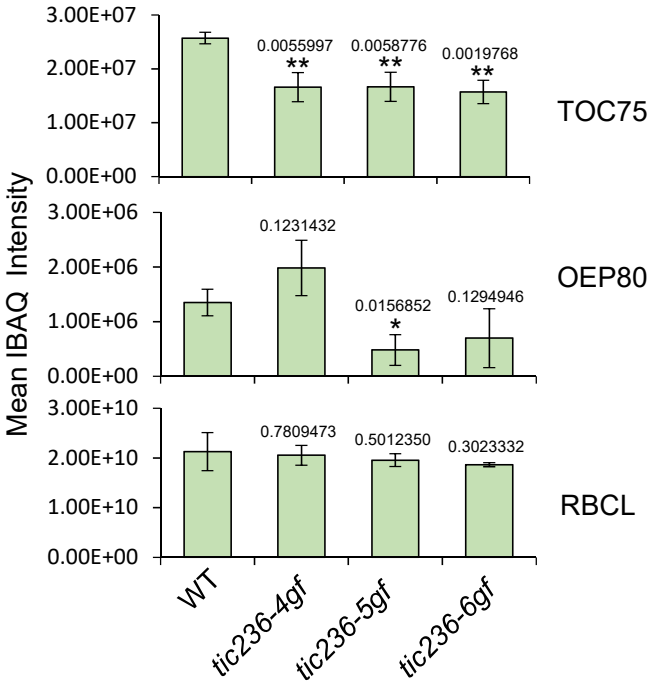

Figure S7. Label-free protein quantitation of TOC75 and OEP80 proteins in *tic236-gf* plants. iBAQ intensities are shown as mean ± SD (n=3). Ribulose-bisphosphate carboxylase large-chain (RBCL) was chosen as the control. All *P*-values are from two-tailed Student's *t*-tests. *$P < 0.05$, **$P < 0.01$.

ID	Gene	Name	Primer sequence (5' to 3')	Purpose
AT5G51020	CRL	crl-LP	CCGAGAGACGTGAGATCAGT	Genotyping
		crl-RP	ggtcacCTGTTCGAGATACA	
AT5G53170	FTSH11	ftsh11-1-LP	CTCCTCTCCATACTTCTTCGT	
		ftsh11-1-RP	agtcatggtaacaatacCAGT	
AT5G53170	FTSH11	ftsh11-2-LP	AAGCAACCACTGCATGTTACC	
		ftsh11-2-RP	TGTCTTTCCAGTACCAGGTGC	
AT1G63900	SP1	sp1-3-LP	TATTCGCTGAATCGAGCAAAC	
		sp1-3-RP	GCTGCCATGTATAACAGGCTG	
AT2G25660	TIC236	tic236-2-LP	GTTGTGTAATCCACGCACATG	
		tic236-2-RP	ACGAAACGCCCTTCTAGCTAC	
AT2G25660	TIC236	M4 seq F	GTTGCTCTCCTTTTCTCTTC	Sequencing to identify TIC236-4GF mutation
		M4 seq R	CGAATTACAGACAACAGGCCA	
AT2G25660	TIC236	M5 seq F	CTAAATCTTCAGAAGCGAAGAG	Sequencing to identify TIC236-5GF mutation
		M5 seq R	GGCAATACATATTCACCTTGAA	
AT2G25660	TIC236	M6 seq F	TTGACTTCCATGGAGATGATTGG	Sequencing to identify TIC236-6GF mutation
		M6 seq R	TGGTGACAAGAGTTTCCTCAAAGA	
AT3G18780	ACT2	Q ACTIN2 F	CTGTTGACTACGAGCAGGAGATGG	qRT-PCR
		Q ACTIN2 R	CAAACGAGGGCTGGAACAAGACT	
AT2G37760	AKR4C8	Q AKR4C8 F	CGGCTGTTAACCAAGTTGAATG	
		Q AKR4C8 R	CCCAAAGGAGAGTAACCAGATAAG	
AT1G77120	ADH1	Q ADH1 F	GAGTGTGTGAACCCGAAAGA	
		Q ADH1 R	GTAGTTCCCGAAGAAAGTACCC	
AT3G27630	SMR7	Q SMR7 F	CGCCAAAACATCGATTCGGG	
		Q SMR7 R	TCGAAATCTGAAGGAGGCACA	
AT1G70440	SRO3	Q SRO3 F	CGGTTGGTACTCTGGTTCTAAA	
		Q SRO3 R	GCGAGAGAGTAACGATGATGAA	
AT5G51020	CRL	attb-CRL-F	GGGGACAAGTTTGTACAAAAAAGCAGGCTtc ATGGGTACCGAGTCGGGTTC	Generate CRL fragment for BiFC construct
		attb-CRL-R	GGGGACCACTTTGTACAAGAAAGCTGGGTc GTCTTGCAAGATGAGGGACCC	
AT1G02280	TOC33	attb-TOC33-F	GGGGACAAGTTTGTACAAAAAAGCAGGCTtc ATGGGGTCTCTCGTTCGTGA	Generate TOC33 fragment for BiFC construct
		attb-TOC33Ter-R	GGGGACCACTTTGTACAAGAAAGCTGGGTc TTAAAGTGGCTTTCCACTTGT	
AT5G05000	TOC34	attb-TOC34-F	GGGGACAAGTTTGTACAAAAAAGCAGGCTT CATGGCAGCTTTGCAAACGCTTCGT	Generate TOC34 fragment for BiFC construct
		attb-TOC34Ter-R	GGGGACCACTTTGTACAAGAAAGCTGGGTC TCAAGACCTTCGACTTGCTAAACC	
AT1G67090	RBCS1A	attb-mRbcSatg-F	GGGGACAAGTTTGTACAAAAAAGCAGGCTT CATGGAATTGGCTAAGGAAGTTGACT	Generate mRBCS fragment for BiFC construct
		attb-mRbcS-R	GGGGACCACTTTGTACAAGAAAGCTGGGTC ACCGGTGAAGCTTGGTGGC	
AT5G55280	FTSZ1	attb-mFtsZ1atg-F	GGGGACAAGTTTGTACAAAAAAGCAGGCTT CATGTCCTTCTCTCCGATGGAATCTGCG	Generate mFTSZ1 fragment for BiFC construct
		attb-mFtsZ1-R	GGGGACCACTTTGTACAAGAAAGCTGGGTC GAAGAAAAGTCTACGGGGAGAAGACGA	
AT2G36250	FTSZ2-1	attb-mFtsZ2-1atg-F	GGGGACAAGTTTGTACAAAAAAGCAGGCTT CATGGCCGCTCAGAAATCTGAATC	Generate mFTSZ2-1 fragment for BiFC construct
		attb-mFtsZ2-1-R	GGGGACCACTTTGTACAAGAAAGCTGGGTC GACTCGGGGATAACGAGAG	
AT3G52750	FTSZ2-2	attb-mFtsZ2-2atg-F	GGGGACAAGTTTGTACAAAAAAGCAGGCTT CATGGCTTCTCATAAGTACGAGTCTTC	Generate mFTSZ2-2 fragment for BiFC construct
		attb-mFtsZ2-2-R	GGGGACCACTTTGTACAAGAAAGCTGGGTC GAGGCGAGGATAGCGAGAGC	

AT5G55280	FTSZ1	attb-FtsZ1tp-F	GGGGACAAGTTTGTACAAAAAAGCAGGCTT CATGGCGATAATTCCGTTAGCA	Generate tpFTSZ1 fragment for BiFC construct
		attb-FtsZ1tp-R	GGGGACCACTTTGTACAAGAAAGCTGGGTC TGTTGAATCGCTTCTTCGTTT	
AT2G36250	FTSZ2-1	attb-FtsZ2-1tp-F	GGGGACAAGTTTGTACAAAAAAGCAGGCTT CATGGCAACTTACGTTTCACC	Generate tpFTSZ2-1 fragment for BiFC construct
		attb-FtsZ2-1tp-R	GGGGACCACTTTGTACAAGAAAGCTGGGTC AACAACAACTCGGTTTTTCTTAC	
AT3G52750	FTSZ2-2	attb-FtsZ2-2tp-F	GGGGACAAGTTTGTACAAAAAAGCAGGCTT CATGGCAGCTTATGTTTCTCC	Generate tpFTSZ2-2 fragment for BiFC construct
		attb-FtsZ2-2tp-R	GGGGACCACTTTGTACAAGAAAGCTGGGTC AACAACACGATATCTTTTAGTAG	
AT1G67090	RBCS1A	attb-RbcStp-F	GGGGACAAGTTTGTACAAAAAAGCAGGCTT CATGGCTTCCTCTATGCTCTCT	Generate tpRBCS fragment for BiFC construct
		attb-RbcStp-R	GGGGACCACTTTGTACAAGAAAGCTGGGTC GGAATCGGTAAGGTCAGGAAG	

Table S1: List of primers used in this study.

Dataset S1 (separate file). The expresson levels of genes upregulated in 5-day-old seedlings of *crl* versus WT are shown in *spcrl1*.

Dataset S2 (separate file). The expresson levels of genes downregulated in 5-day-old seedlings of *crl* versus WT are shown in *spcrl1*.

Dataset S3 (separate file). List of the proteins that were found to be associated with CRL.

Dataset S4 (separate file). List of TOC, TIC, and plastid division proteins that may associate with CRL.

Dataset S5 (separate file). iBAQ intensity of TOC and TIC proteins in *tic236gf* mutants versus WT.